ELSEVIER

NeuroImage

www.elsevier.com/locate/ynimg
NeuroImage 26 (2005) 822–828

Mean diffusivity and fractional anisotropy histogram analysis of the cervical cord in MS patients

Paola Valsasina,[a] Maria A. Rocca,[a,b] Federica Agosta,[a,b] Beatrice Benedetti,[a,b] Mark A. Horsfield,[c] Antonio Gallo,[a] Marco Rovaris,[a,b] Giancarlo Comi,[b] and Massimo Filippi[a,b,*]

[a]*Neuroimaging Research Unit, Department of Neurology, Scientific Institute and University Ospedale San Raffaele, Via Olgettina, 60, 20132 Milan, Italy*
[b]*Department of Neurology, Scientific Institute and University Ospedale San Raffaele, Milan, Italy*
[c]*Department of Cardiovascular Sciences, University of Leicester, Leicester Royal Infirmary, United Kingdom*

Received 26 October 2004; revised 25 January 2005; accepted 17 February 2005
Available online 31 March 2005

The spinal cord is frequently involved in multiple sclerosis (MS), and cord damage may be an important contributor to disability. Diffusion tensor magnetic resonance imaging (DT-MRI) provides quantitative information about the structural and orientational features of the central nervous system. In order to assess whether diffusion tensor-derived measures of cord tissue damage are related to clinical disability, mean diffusivity (MD) and fractional anisotropy (FA) histograms from the cervical cord were acquired from a large cohort of MS patients. Diffusion-weighted sensitivity-encoded (SENSE) echo planar images of the cervical cord, and brain dual-echo and diffusion-weighted scans were acquired from 44 patients with MS and 17 healthy controls. Cord and brain MD and FA histograms were produced. An analysis of variance model, adjusting for cord volume and patient age, was used to compare cord DT-MRI parameters from controls and patients. A multivariate linear regression model was used to identify DT-MRI variables independently associated with disability. Average cervical cord FA was significantly lower in MS patients compared to controls. Cord cross-sectional area, average FA and average MD were all significantly correlated with the degree of disability (r values ranging from 0.36 to 0.51). The multivariate linear regression model retained average cord FA and average brain MD as variables independently associated with disability, with a correlation coefficient of 0.73 ($P < 0.001$). DT-MRI reveals a loss of cervical cord tissue structure in MS patients. The strong correlation found between a composite DT-MRI score and disability suggests that a full and accurate assessment of cervical cord damage in MS provides information that usefully contributes to an explanation of the clinical manifestations of the disease.

Keywords: Mean diffusivity; Fractional anisotropy; Multiple sclerosis; DT-MRI; Spinal cord

Introduction

The spinal cord is a clinically eloquent site, which is frequently involved in multiple sclerosis (MS) (Ikuta and Zimmermann, 1976). A post-mortem study showed cord lesions in 86% of patients with MS (Ikuta and Zimmermann, 1976), and magnetic resonance imaging (MRI) cord abnormalities are detected in 47% to 90% of patients with established disease (Hittmair et al., 1996; Kidd et al., 1993; Lycklama à Nijeholt et al., 1998; Rocca et al., 1999; Stevenson et al., 1998a,b; Tartaglino et al., 1995). However, previous studies have failed to show a significant correlation between the number and extent of spinal cord lesions seen on conventional T_2-weighted MRI scans and MS disability (Kidd et al., 1993; Stevenson et al., 1998a,b). This is likely to be a consequence of the limitations of conventional MRI, which lacks specificity to the heterogeneous pathological substrates of MS, and does not provide information about normal appearing white matter damage (Filippi, 1998).

Diffusion-tensor (DT) MRI enables the random diffusional motion of water molecules to be measured and provides quantitative indices of the structural and orientational features of tissues (Pierpaoli et al., 1996). These indices include mean diffusivity (MD), which is a directionally averaged measure of the apparent diffusion coefficient, and fractional anisotropy (FA), which summarizes the orientational dependence of diffusivity. The pathological elements of MS have the potential to alter the permeability and geometry of structural barriers to water molecular diffusion in the

* Corresponding author. Neuroimaging Research Unit, Department of Neurology, Scientific Institute and University Ospedale San Raffaele, Via Olgettina, 60, 20132 Milan, Italy. Fax: +39 02 2643 3054.
E-mail address: m.filippi@hsr.it (M. Filippi).
Available online on ScienceDirect (www.sciencedirect.com).

1053-8119/$ - see front matter © 2005 Elsevier Inc. All rights reserved.
doi:10.1016/j.neuroimage.2005.02.033

central nervous system (CNS). The application of DT-MRI to MS is, therefore, appealing since it can provide quantities related of the degree of tissue damage and, as a consequence, could improve our understanding of the mechanisms leading to irreversible disability. While DT-MRI has been widely applied to study the brains of MS patients (Filippi et al., 2003), DT-MRI of the cord presents greater technical challenges due to the small size of this structure and artefacts related to magnetic field inhomogeneities, cerebrospinal fluid (CSF) contamination and cardiac and respiratory motion (Clark and Werring, 2002; Clark et al., 2000; Mottershead et al., 2003; Wheeler-Kingshott et al., 2002). As a consequence, spinal cord DT-MRI has only been applied in a preliminary study of three MS patients (Clark et al., 2000), which has shown, using a region of interest (ROI) analysis, increased MD and decreased anisotropy in MS cord lesions (Clark et al., 2000).

A more global evaluation of the extent and severity of cervical cord damage with DT-MRI might provide a more complete picture of cord damage in MS and, as a consequence, might improve our ability to monitor MS. In this study, we obtained MD and FA histograms of a large portion of the cervical cord from a cohort of MS patients to investigate the magnitude of the correlation between diffusion histogram-derived metrics and patients' disability.

Patients and methods

Patients

We studied 44 patients with definite MS (McDonald et al., 2001) (33 women and 11 men; mean age = 38.9 years, SD = 9.6 years); median disease duration = 9 years, range = 1–27 years; median Expanded Disability Status Scale (EDSS) score (Kurtzke, 1983) = 4.5, range = 1.0–7.5). Twenty-one patients had relapsing–remitting MS (RRMS) and 23 secondary progressive MS (SPMS) (Lublin and Reingold, 1996). The demographic and clinical characteristics of the two groups of patients are presented in Table 1. Seventeen sex- and age-matched healthy volunteers (12 women and 5 men; mean age = 35.5 years, SD = 11.4 years) with no history of neurological disorders and a normal neurological examination served as controls. Local Ethical Committee approval and written informed consent from all individuals were obtained before study initiation.

Image acquisition

Using a 1.5 T system (Magnetom Vision, Siemens, Erlangen, Germany), the following pulse sequences were acquired from the cervical cord of all subjects, using a tailored cervical spine phased array coil for signal reception:

(1) Fast-short-tau inversion recovery (fast-STIR) (TR = 2288, TE = 60, TI = 110, ETL = 11, FOV = 280 × 280 mm, matrix size = 264 × 512, number of signal averages = 4; number of slices = 8; sagittal plane; slice thickness = 3 mm; inter-slice gap = 0.3 mm).
(2) Pulsed-gradient, diffusion-weighted (DW) sensitivity encoded (SENSE) single-shot EPI (reduction factor, R = 2; TR = 7000, TE = 100; FOV = 240 × 90 mm; matrix = 128 × 48; echo train = 40 ms; number of slices = 5; sagittal plane; slice thickness = 4 mm). This sequence collects 16 images per section, including two images with no diffusion weighting ($b \approx 0$ s/mm^2) and 14 images with the same b factor of 900 s mm^{-2}, but with gradients applied in different directions. The non-diffusion-weighted images are needed to compute the diffusion tensor, and the gradient orientations were chosen according to the algorithm proposed by Jones et al. (1999), which was designed to optimize DT-MRI acquisition. The measurement was repeated four times to improve the signal-to-noise ratio (SNR). Three saturation bands were used, positioned in the anterior part of the neck and transversely at the edges of the FOV in the superior–inferior direction. A detailed description of this sequence is given elsewhere (Cercignani et al., 2003).
(3) Sagittal T_1-weighted 3D magnetization-prepared rapid acquisition gradient echo (MP-RAGE) sequence (TR = 9.7, TE=4, flip angle = 12°, slab thickness = 160 mm, FOV = 280 × 280 mm, number of partitions = 128).

In the same scanning session, the following pulse sequences were used to image the brain using a birdcage head coil of ~300 mm diameter for RF transmission and signal reception:

(1) Dual-echo turbo spin echo (TSE) (TR = 3300, TE first echo = 16, TE second echo = 98, echo train length = 5).
(2) Pulsed-gradient DW EPI (inter-echo spacing = 0.8, TE = 123), with diffusion-weighting gradients applied in 8 different directions (Filippi et al., 2001). As in the cervical cord, only two b factors were used: $b_1 \approx 0$, and b_2 = 1044 s mm^{-2} (Bito et al., 1995).

For the TSE, 24 contiguous interleaved axial slices were acquired with 5 mm slice thickness, 256 × 256 matrix and 250 × 250 mm FOV. The slices were positioned to run parallel to a line that joins the most infero-anterior and infero-posterior parts of the corpus callosum. For the DW scans, 10 axial slices with 5 mm slice thickness, 128 × 128 matrix and 250 × 250 mm FOV were acquired, with the same orientation as the dual echo scans, and with the second-last caudal slice positioned to match exactly the central slices of the dual-echo set. This brain portion was chosen since these central slices are less affected by the distortions due to B_0 field inhomogeneity, which can affect image co-registration.

Image analysis

All MRI analysis was performed by two experienced observers by consensus, unaware to whom the scans belonged. Cervical cord

Table 1
Main demographic and clinical characteristics of the MS patients studied

	RRMS	SPMS	P[a]
Mean age (SD) [years]	33.1 (6.2)	43.9 (9.6)	0.001
Median disease duration (range) [years]	6.0 (1.0–13.0)	12.0 (4.0–37.0)	$P < 0.0001$
Median EDSS (range)	2.5 (1.0–5.5)	6.0 (3.0–7.5)	$P < 0.0001$

MS = multiple sclerosis, RR = relapsing remitting, SP = secondary progressive, SD = standard deviation, EDSS = expanded disability status scale score.
[a] Two-tailed Student's t test for not-paired data.

Table 2
Means and ranges of intra-observer coefficients of variation of cord DT-MRI quantities

	CoV	Ranges
Average MD	1.2%	0.1–3.1%
MD peak height	7.7%	4.8–11.9%
Average FA	2.7%	0.6–6.8%
FA peak height	8.7%	3.4–10.8%

CoV = coefficient of variation, MD = mean diffusivity, FA = fractional anisotropy.

hyperintense lesions were identified on the fast-STIR scans and marked on the hardcopies. Cervical cord DT-MRI data were reconstructed offline, as described by Pruessmann et al. (1999). Once the wrapping in the phase-encoded direction was corrected, the diffusion-weighted images were magnitude averaged to improve the SNR. The images were then corrected for distortions introduced by the DW gradient pulses, as previously described (Cercignani et al., 2003). The DT was calculated for each voxel by using linear regression (Basser et al., 1994), and the eigenvalues and eigenvectors of the tensor matrix were derived. The eigenvalues were averaged to give the MD and used to calculate the FA (Pierpaoli and Basser, 1996).

From cervical cord MD and FA maps, the cord from C1 to C5 was segmented using a segmentation technique, which has been described previously (Rovaris et al., 1997). The influence of signal intensity artefacts at the edges of the images was carefully excluded. To reduce partial volume effects from the CSF, only the central slice of the sagittal images was used for the analysis.

Hyperintense brain lesions were identified on the proton-density (PD) weighted scans and marked on the hardcopies. The corresponding T_2-weighted images were always used to increase confidence in lesion identification. Then, lesion volumes were measured using a segmentation technique based on local thresholding, as previously described (Rovaris et al., 1997). DW images were first corrected for distortions introduced by DW gradient pulses using an algorithm which maximizes mutual information between the diffusion un-weighted and weighted images (Studholme et al., 1997). Then, the diffusion tensor was calculated, and MD and FA derived for every pixel, as for the cord.

The final step of MD and FA analysis was the production of brain and cervical cord histograms (bin width of 0.03×10^{-3} mm^2 s^{-1} for MD histogram and of 0.01 for FA histogram). To correct for the between-patient differences in cord and brain volume, each histogram was normalized by dividing the height of each histogram bin by the total number of pixels included. For each histogram, the following measures were derived: the average MD and FA and the histogram peak height. To test intra-observer reproducibility, a single observer segmented the cord tissue twice from all the healthy volunteers. MD and FA metrics were then derived. For each metric, the intra-observer variability was calculated by using the coefficient of variation (CoV), defined as the standard deviation of a random variable divided by its mean value.

Reformatting of the original MP-RAGE data was performed using the standard, vendor-supplied multiplanar reformatting software available on the operator's console of the scanner. For each subject, a set of five contiguous, 3-mm thick axial slices (perpendicular to the spinal cord) was reconstructed using the center of the C2–C3 disc as the caudal landmark. Then, a semi-automated technique developed by Losseff et al. (1996) was used to segment the cord tissue and to measure the cross-sectional cord area at the level of each slice. Values from the five slices were averaged to obtain a single value for each subject.

Statistical analysis

An analysis of variance model with a priori contrasts was used to compare the cervical cord and brain DT-MRI histogram parameters from controls and patients with different clinical phenotypes. The analyses of cervical cord DT-MRI derived metrics were corrected by including in the model the subject's age and the mean cross-sectional cord area to minimize the effect of cord atrophy on such metrics. The analysis of brain DT-MRI derived metrics was also corrected for subject's age. The following a priori contrasts were chosen: control subjects vs. MS patients and RRMS vs. SPMS. The number of the a priori contrasts was determined by the available degrees of freedom, and their nature was chosen on the basis of clinical considerations. Univariate correlations were assessed using the Spearman rank correlation coefficient (SRCC). A multivariate linear regression model was used to identify MRI variables independently correlated with the EDSS (rank transformed). To this end, all the MRI variables significantly correlated with the EDSS in the univariate analysis were included in the model. The variables retained in the final model were correlated with the EDSS using the SRCC.

Results

No abnormalities were seen on the conventional brain and cervical cord MR images obtained from normal volunteers. Hyperintense lesions on fast-STIR scans of the cord were detected in 35 MS patients (15 patients with RRMS and 20 patients with SPMS). The median number of lesions per patient was 2 (range = 0–5). No difference was found in the number of cervical cord lesions between patients with RRMS and those with SPMS (data not shown).

Table 3
Cervical cord MD and FA histogram-derived metrics from MS patients and controls

	Control subjects	All MS patients	RRMS	SPMS	P^a
Average MD (SD)	1.222 (0.08)	1.282 (0.13)	1.256 (0.10)	1.304 (0.14)	0.9
MD peak height (SD)	107.3 (16.2)	105.7 (21.2)	110.7 (19.2)	101.1 (22.3)	0.7
Average FA (SD)	0.43 (0.03)	0.36 (0.06)	0.39 (0.05)	0.34 (0.05)	0.01
FA peak height (SD)	63.6 (16.5)	65.7 (13.5)	66.3 (11.7)	65.2 (15.1)	0.2

SD = standard deviation, MD = mean diffusivity, FA = fractional anisotropy, MS = multiple sclerosis, RR = relapsing remitting, SP = secondary progressive. *Note*. Average MD of the diffusivity histogram is expressed in units of mm^2 s^{-1} $\times 10^{-3}$; FA is a dimensionless index, MD and FA peak heights are multiplied by $\times 10^3$.

[a] Test for heterogeneity between groups corrected for cord cross-sectional area and age (see text for further details).

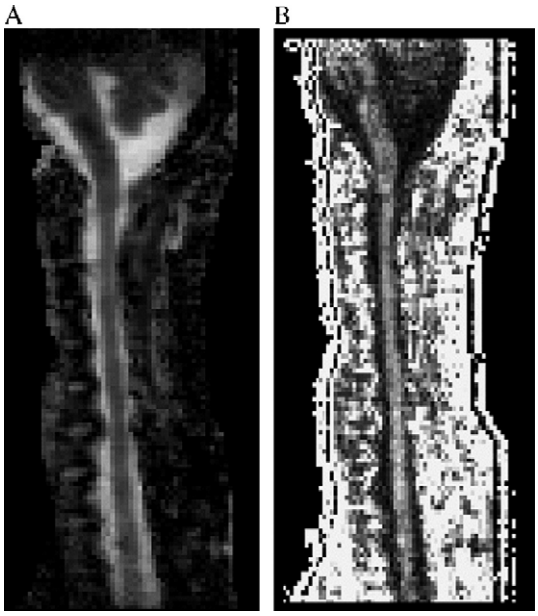

Fig. 1. Sagittal mean diffusivity (A) and fractional anisotropy maps (B) obtained from a patient with relapsing remitting MS. In this patient, who was mildly disabled, cord anisotropy is clearly preserved (B).

In MS patients, dual-echo lesion load in the brain was 18.6 ml (SD = 17.1). It was 16.4 ml (SD = 18.1 ml) in RRMS patients and 21.0 ml (SD = 16.1 ml) in SPMS patients (P = n.s.).

The mean values and ranges of the intra-observer CoVs for the cord diffusivity metrics are reported in Table 2.

In Table 3, cervical cord DT-MRI histogram metrics from healthy volunteers and MS patients are reported. In Fig. 1, an example of a MD and FA maps obtained from a patient with RRMS is shown. Cervical cord cross-sectional area was 84.9 mm^2 (SD = 10.2 mm^2) in healthy volunteers and 76.4 mm^2 (SD = 13.2 mm^2) in MS patients ($P = 0.03$). Cervical cord cross-sectional area was significantly lower in SPMS (mean area = 70.7 mm^2; SD = 12.6 mm^2) than in RRMS (mean area = 82.6 mm^2; SD = 11.1 mm^2) patients ($P = 0.002$). Average cervical cord FA was also significantly different among the three study groups ($P = 0.01$). MS patients had significantly lower average cord FA than healthy volunteers ($P = 0.008$), but no difference was found between RRMS and SPMS patients ($P = 0.20$). In Fig. 2, the average MD and FA histograms from control subjects, RRMS and SPMS patients are shown.

Average brain MD, MD peak height and average brain FA were significantly different between groups (Table 4); the contrasts between controls and all MS patients were significant for all these variables ($P < 0.001$), while there was a significant difference between RRMS and SPMS patients for MD only ($P = 0.02$).

In the entire MS patient cohort, significant univariate correlations were found between EDSS score and cord cross-sectional area ($r = -0.51$, $P = 0.001$), average cord FA ($r = -0.48$, $P = 0.001$) and average cord MD ($r = 0.36$, $P = 0.02$). EDSS score was also significantly correlated with average brain MD ($r = 0.37$, $P = 0.02$) and average brain FA ($r = -0.35$, $P = 0.03$). No significant correlations were found between cord DT-MRI histogram derived metrics and conventional and DT-MRI metrics derived from the brain (data not shown).

A multivariate regression model with EDSS as the dependent variable was run, including cord mean cross-sectional area, average cord FA, average cord MD, average brain FA and average brain MD as the independent variables. The final model retained average cord FA ($P < 0.001$) and average brain MD ($P = 0.02$) as variables influencing independently the EDSS score. The correlation with EDSS of the composite score obtained combining these two variables was 0.73 ($P < 0.001$).

Discussion

Involvement of the spinal cord, a common finding in MS (Hittmair et al., 1996; Ikuta and Zimmermann, 1976; Kidd et al., 1993; Lycklama à Nijeholt et al., 1998; Rocca et al., 1999; Stevenson et al., 1998a,b; Tartaglino et al., 1995), is likely to contribute to the accumulation of disability, particularly locomotor impairment, which is one of the main clinical hallmarks of the progressive phenotypes of the disease. However, previous studies found no correlations between the number and extent of lesions visible on conventional MRI and clinical disability (Kidd et al., 1993; Lycklama à Nijeholt et al., 1998; Stevenson et al., 1998a,b). This discrepancy is most likely the result of the inability of conventional MRI to quantify accurately the degree of cord tissue

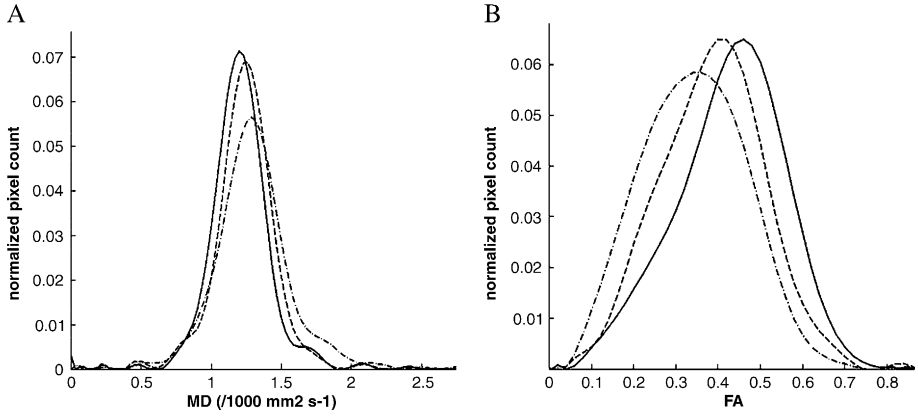

Fig. 2. Average MD (A) and FA (B) histograms of the cervical cord from healthy controls (continuous lines), patients with RRMS (dashed lines) and patients with SPMS (dashed-dotted lines). See the text for further details. Note that these average histograms do not necessarily show the same trend as the statistics presented in Table 2, because the average histogram also reflects the differences in the position of the peak of the histogram among patients.

Table 4
Brain MD and FA histogram-derived measures from MS patients and controls

	Control subjects	All MS patients	RRMS	SPMS	P^a
Average MD (SD)	0.901 (0.05)	1.001 (0.09)	0.990 (0.09)	1.011 (0.10)	0.001
MD peak height (SD)	121.3 (14.6)	91.6 (19.7)	93.4 (18.7)	89.9 (21.1)	<0.001
Average FA (SD)	0.22 (0.01)	0.20 (0.02)	0.20 (0.01)	0.19 (0.02)	0.002
FA peak height (SD)	46.2 (4.18)	47.7 (3.82)	47.4 (3.56)	48.0 (4.14)	0.2

SD = standard deviation, MD = mean diffusivity, FA = fractional anisotropy, MS = multiple sclerosis, RR = relapsing remitting, SP = secondary progressive.
Note. Average MD of the diffusivity histogram is expressed in units of $mm^2\ s^{-1} \times 10^{-3}$, FA is a dimensionless index, MD and FA peak heights are multiplied by $\times 10^3$.
[a] Test for heterogeneity between groups corrected for age (see text for further details).

damage. As in the brain (Allen and McKeown, 1979; Arstila et al., 1973; Evangelou et al., 2000), post-mortem studies have shown convincingly that cord damage is not limited to macroscopic lesions visible on conventional images (Bergers et al., 2002; DeLuca et al., 2004; Lovas et al., 2000). Widespread axonal loss has indeed been detected in the spinal cord of MS patients, which was independent of findings on T_2-weighted scans (Bergers et al., 2002; Lovas et al., 2000). These changes were found to be more severe in the cervical portion of the cord and in patients with SPMS (Lovas et al., 2000). Loss of axons is likely to be the pathological substrate of cord atrophy, often observed in these patients (Lycklama et al., 2003).

While the recent application of DT-MRI to the brain in MS has helped in our understanding of the pathophysiology of the disease (Filippi et al., 2003), at present, only one study has been performed to assess, in vivo, the diffusivity characteristics of the cervical cord of three MS patients (Clark et al., 2000). Using an ROI analysis, Clark et al. (2000) found increased MD and reduced FA values in T_2-visible lesions of MS patients compared to normal cord white matter of healthy subjects. This study was limited by the very small sample of patients studied and by ROI analysis, which is operator-dependent, has poor reproducibility and is unable to provide an estimate of the overall disease-related damage in the cord. On the other hand, histogram analysis provides multiple parameters influenced by both the macro- and microscopic damage, thus resulting in a more global picture of the disease burden in MS patients. The application of DT-MRI histogram analysis to the assessment of brain pathology in MS has shown that DT-MRI histogram-derived metrics from MS patients are altered when compared to healthy individuals and that these abnormalities vary according to the disease phenotype (Filippi et al., 2001, 2003). The findings from the brain, from the current study, agree with these previous observations and show that DT-MRI of the brain gives an important contribution to the understanding of MS pathology, which is not overcome by the assessment of cord diffusivity, perhaps because of the multifocal nature of the disease coupled with the technical limitations, which are still associated to cord imaging.

The novelty of this study lies in the demonstration that it is both feasible and rewarding in terms of understanding MS pathobiology to obtain MD and FA histograms of the cervical cord. Since cervical cord atrophy is a frequent finding in MS (Filippi et al., 1996; Lycklama et al., 2003; Nijeholt et al., 2001; Stevenson et al., 1998b) as also shown by the present study, and since, when atrophy is present, there is an increased likelihood of partial volume effect from the CSF on the MD and FA histograms derived metrics, we ran the a priori contrast analysis with correction for cord cross-sectional area. Contamination from the CSF was further minimized by considering in the analysis only pixels coming from the central slice of the sagittal slab and by including only pixels from C1 to C5. This inevitably was at the price of restricting the portion of the cervical cord studied, but we believe that it made our observations more robust and reliable. This is confirmed by the results of the analysis of intra-observer reproducibility, which match those obtained in a previous MTR study of the brain (Sormani et al., 2000).

In line with previous studies (Filippi et al., 1996; Losseff et al., 1996), we found that cord atrophy is correlated with the level of disability in MS. However, the most intriguing finding of this study was that the residual cord tissue is not spared by MS pathology and that an important factor which is likely to cause permanent disability in MS is loss of integrity of fiber bundles, as indicated by the correlation found between the reduction in average cord FA and the EDSS score.

We found that, in comparison to healthy subjects, MD of the cervical cord of MS patients was increased (albeit not significantly) and that FA was markedly reduced. In the light of the results of a recent post-mortem study (Mottershead et al., 2003), which demonstrated a strong correlation between axonal density in the spinal cord of MS patients with decreased diffusion anisotropy but only a weak correlation with increased apparent diffusion coefficient, our findings suggest that reduced cord FA reflects a loss of the alignment of nerve fibers in the cord of MS patients, which in turn is likely to be the result of axonal pathology. The partial mismatch between MD and FA findings might be secondary to glial proliferation (Nijeholt et al., 2001), which would lead to a "pseudo-normalization" of MD values, but which would reduce FA, since glial cells do not have the same anisotropic morphology as the tissue they replace. With this in mind, an important issue is whether the cord axonal pathology results from intrinsic cord damage or rather is secondary to Wallerian degeneration of long fiber tracts passing through brain lesions. Although this study can only give a partial answer to this question, it is likely that anterograde degeneration does not play a major role, given the lack of a correlation between cord and brain metrics, which is consistent with the results of previous studies (Lycklama à Nijeholt et al., 1998; Rovaris et al., 2000).

The discrepancy between our DT-MRI findings of the cord (markedly reduced FA but only mildly increased MD) and previous findings obtained from DT-MRI assessment of brain pathology (reduced FA and increased MD at a similar magnitude) (Filippi et al., 2003) is likely due to the different anatomical organization of these two structures: cord fibers are indeed highly compact with a definite direction (cranial/caudal or caudal/cranial), thus resulting in a marked tissue anisotropy, whereas brain fibers bundles are more heterogeneous in terms of direction and also the amount of gray matter regions is much higher than in the cord. All of this is likely to limit the ability to detect marked FA changes in the brain.

Using a composite MR model, in which brain and cord measures reflecting the severity of MS-related abnormalities were combined, we found that the degree of tissue damage in the cord (expressed as average FA) and in the brain (expressed as average MD) independently influenced the EDSS. The independent contributions of brain MD and cord FA are likely to be the result of the different sensitivity of these two quantities in detecting irreversible tissue damage in the brain and cord, which, in turn, might be due to the different white matter fiber geometry of these CNS structures. Taken together, these variables help to explain about 50% of the variance of patients' disability. Although this observation needs to be replicated in other diffusion studies, these results, combined with those of previous studies performed using different MR-based techniques (Mainero et al., 2001; Rovaris et al., 2001), suggest that the use of an MRI composite score, in which the extent of brain and cord damage is quantified through the combination of various MR modalities, might be the best way to more accurate monitoring of MS.

Acknowledgment

We wish to thank Dr. Maria Pia Sormani for her help in conducting the statistical analysis.

References

Allen, I.V., McKeown, S.R., 1979. A histological, histochemical and biochemical study of the macroscopically normal white matter in multiple sclerosis. J. Neurol. Sci. 41, 81–91.

Arstila, A.U., Riekkinen, P., Rinne, U.K., Laitinen, L., 1973. Studies on the pathogenesis of multiple sclerosis. Participation of lysosomes on demyelination in the central nervous system white matter outside plaques. Eur. Neurol. 9, 1–20.

Basser, P.J., Mattiello, J., LeBihan, D., 1994. Estimation of the effective self-diffusion tensor from the NMR spin echo. J. Magn. Reson., B 103, 247–254.

Bergers, E., Bot, J.C., De Groot, C.J., Polman, C.H., Lycklama a Nijeholt, G.J., Castelijns, J.A., et al., 2002. Axonal damage in the spinal cord of MS patients occurs largely independent of T_2 MRI lesions. Neurology 59, 1766–1771.

Bito, Y., Hirata, S., Yamamoto, E., 1995. Optimal gradient factors for ADC measurements [abstract]. Proc. Int. Soc. Magn. Reson. Med. 2, 913.

Cercignani, M., Horsfield, M.A., Agosta, F., Filippi, M., 2003. Sensitivity-encoded diffusion tensor MR imaging of the cervical cord. AJNR Am. J. Neuroradiol. 24, 1254–1256.

Clark, C.A., Werring, D.J., 2002. Diffusion tensor imaging in spinal cord: methods and application—a review. NMR Biomed. 15, 578–586.

Clark, C.A., Werring, D.J., Miller, D.H., 2000. Diffusion imaging of the spinal cord in vivo: estimation of the principal diffusivities and application to multiple sclerosis. Magn. Reson. Med. 43, 133–138.

DeLuca, G.C., Ebers, G.C., Esiri, M.M., 2004. Axonal loss in multiple sclerosis: a pathological survey of the corticospinal and sensory tracts. Brain 127, 1009–1018.

Evangelou, N., Konz, D., Esiri, M.M., Smith, S., Palace, J., Matthews, P.M., 2000. Regional axonal loss in the corpus callosum correlates with cerebral white matter lesion volume and distribution in multiple sclerosis. Brain 123, 1845–1849.

Filippi, M., 1998. The role of non-conventional magnetic resonance techniques in monitoring the evolution of multiple sclerosis. J. Neurol., Neurosurg. Psychiatry 64 (Supp:1), 52–58.

Filippi, M., Campi, A., Colombo, B., Pereira, C., Martinelli, V., Baratti, C., et al., 1996. A spinal cord MRI study of benign and secondary progressive multiple sclerosis. J. Neurol. 243, 502–505.

Filippi, M., Cercignani, M., Inglese, M., Horsfield, M.A., Comi, G., 2001. Diffusion tensor magnetic resonance imaging in multiple sclerosis. Neurology 56, 304–311.

Filippi, M., Rocca, M.A., Comi, G., 2003. The use of quantitative magnetic-resonance-based techniques to monitor the evolution of multiple sclerosis. Lancet Neurol. 2, 337–346.

Hittmair, K., Mallek, R., Prayer, D., Schindler, E.G., Kollegger, H., 1996. Spinal cord lesions in patients with multiple sclerosis: comparison of MR pulse sequences. AJNR Am. J. Neuroradiol. 17, 1555–1565.

Ikuta, F., Zimmermann, H.M., 1976. Distribution of plaques in seventy autopsy cases of multiple sclerosis in the United States. Neurology 8, 26–28.

Jones, D.K., Horsfield, M.A., Simmons, A., 1999. Optimal strategies for measuring diffusion in anisotropic systems by magnetic resonance imaging. Magn. Reson. Med. 42, 515–525.

Kidd, D., Thorpe, J.W., Thompson, A.J., Kendall, B.E., Moseley, I.F., MacManus, D.G., et al., 1993. Spinal cord MRI using multi-array coils and fast spin echo. II. Findings in multiple sclerosis. Neurology 43, 2632–2637.

Kurtzke, J.F., 1983. Rating neurological impairment in multiple sclerosis: an expanded disability status scale (EDSS). Neurology 33, 1444–1452.

Losseff, N.A., Webb, S.L., O'Riordan, J.I., Page, R., Wang, L., Barker, G.J., et al., 1996. Spinal cord atrophy and disability in multiple sclerosis. A new reproducible and sensitive MRI method with potential to monitor disease progression. Brain 119, 701–708.

Lovas, G., Szilagyi, N., Majtenyi, K., Palkovits, M., Komoly, S., 2000. Axonal changes in chronic demyelinated cervical spinal cord plaques. Brain 123, 308–317.

Lublin, F.D., Reingold, S.C., The national multiple sclerosis society (USA) advisory committee on clinical trials of new agents in multiple sclerosis., 1996. Defining the clinical course of multiple sclerosis: results of an international survey. Neurology 46, 907–911.

Lycklama à Nijeholt, G.J., van Walderveen, M.A.A., Castelijns, J.A., van Waesberghe, J.H., Polman, C., Scheltens, P., et al., 1998. Brain and spinal cord abnormalities in multiple sclerosis. Correlation between MRI parameters, clinical subtypes and symptoms. Brain 121, 687–697.

Lycklama, G., Thompson, A., Filippi, M., Miller, D., Polman, C., Fazekas, F., et al., 2003. Spinal-cord MRI in multiple sclerosis. Lancet Neurol. 2, 555–562.

Mainero, C., De Stefano, N., Iannucci, G., Sormani, M.P., Guidi, L., Federico, A., et al., 2001. Correlates of MS disability assessed in vivo using aggregates of MR quantities. Neurology 56, 1331–1334.

McDonald, W.I., Compston, A., Edan, G., Goodkin, C., Hartung, H.P., Lublin, F., et al., 2001. Recommended diagnostic criteria for multiple sclerosis: guidelines from the international panel on the diagnosis of multiple sclerosis. Ann. Neurol. 50, 121–127.

Mottershead, J.P., Schmierer, K., Clemence, M., Thornton, J.S., Scaravilli, F., Barker, G.J., et al., 2003. High field MRI correlates of myelin content and axonal density in multiple sclerosis. J. Neurol. 250, 1293–1301.

Nijeholt, G.J., Bergers, E., Kamphorst, W., Bot, J., Nicolay, K., Castelijns, J.A., et al., 2001. Post-mortem high-resolution MRI of the spinal cord in multiple sclerosis: a correlative study with conventional MRI, histopathology and clinical phenotype. Brain 124, 154–166.

Pierpaoli, C., Basser, P.J., 1996. Toward a quantitative assessment of diffusion anisotropy. Magn. Reson. Med. 36, 893–906.

Pierpaoli, C., Jezzard, P., Basser, P.J., Barnett, A., Di Chiro, G., 1996. Diffusion tensor MR imaging of the human brain. Radiology 201, 637–648.

Pruessmann, K.P., Weiger, M., Scheidegger, M.B., Boesiger, P., 1999. SENSE: sensitivity encoding for fast MRI. Magn. Reson. Med. 42, 952–962.

Rocca, M.A., Mastronardo, G., Horsfield, M.A., et al., 1999. Comparison of three MR sequences for the detection of cervical cord lesions in multiple sclerosis. AJNR Am. J. Neuroradiol. 20, 1710–1716.

Rovaris, M., Filippi, M., Calori, G., et al., 1997. Intra-observer reproducibility in measuring new putative markers of demyelination and axonal loss in multiple sclerosis: a comparison with conventional T2-weighted images. J. Neurol. 18, 895–901.

Rovaris, M., Bozzali, M., Santuccio, G., et al., 2000. Relative contributions of brain and cervical cord pathology to multiple sclerosis disability: a study with magnetization transfer ratio histogram analysis. J. Neurol. Neurosurg. Psychiatry 69, 723–727.

Rovaris, M., Bozzali, M., Santuccio, G., et al., 2001. In vivo assessment of the brain and cervical cord pathology of patients with primary progressive multiple sclerosis. Brain 124, 2540–2549.

Sormani, M.P., Iannucci, G., Rocca, M.A., Mastronardo, G., Cercignani, M., Minicucci, L., Filippi, M., 2000. Reproducibility of magnetisation transfer ratio histogram-derived measures of the brain in healthy volunteers. AJNR Am. J. Neuroradiol. 21, 133–136.

Stevenson, V.L., Moseley, I.F., Phatouros, C.C., MacManus, D., Thompson, A.J., Miller, D.H., 1998a. Improved imaging of the spinal cord in multiple sclerosis using three-dimensional fast spin echo. Neuroradiology 40, 416–419.

Stevenson, V.L., Leary, S.M., Losseff, N.A., Parker, G.J., Barker, G.J., Husmani, Y., et al., 1998b. Spinal cord atrophy and disability in MS. A longitudinal study. Neurology 51, 234–238.

Studholme, C., Hill, D.L., Hawkes, D.J., 1997. Automated three-dimensional registration of magnetic resonance and positron emission tomography brain images by multiresolution optimization of voxel similarity measures. Med. Phys. 24, 25–35.

Tartaglino, L.M., Friedman, D.P., Flanders, A.E., Lublin, F.D., Knobler, R.L., Liem, M., 1995. Multiple sclerosis in the spinal cord: MR appearance and correlation with clinical parameters. Radiology 195, 725–732.

Wheeler-Kingshott, C.A., Hickman, S.J., Parker, G.J., Ciccarelli, O., Symms, M.R., Miller, D.H., et al., 2002. Investigating cervical spinal cord using axial diffusion tensor imaging. NeuroImage 16, 93–102.